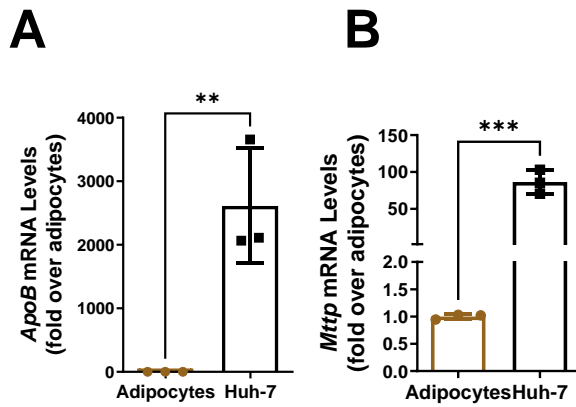
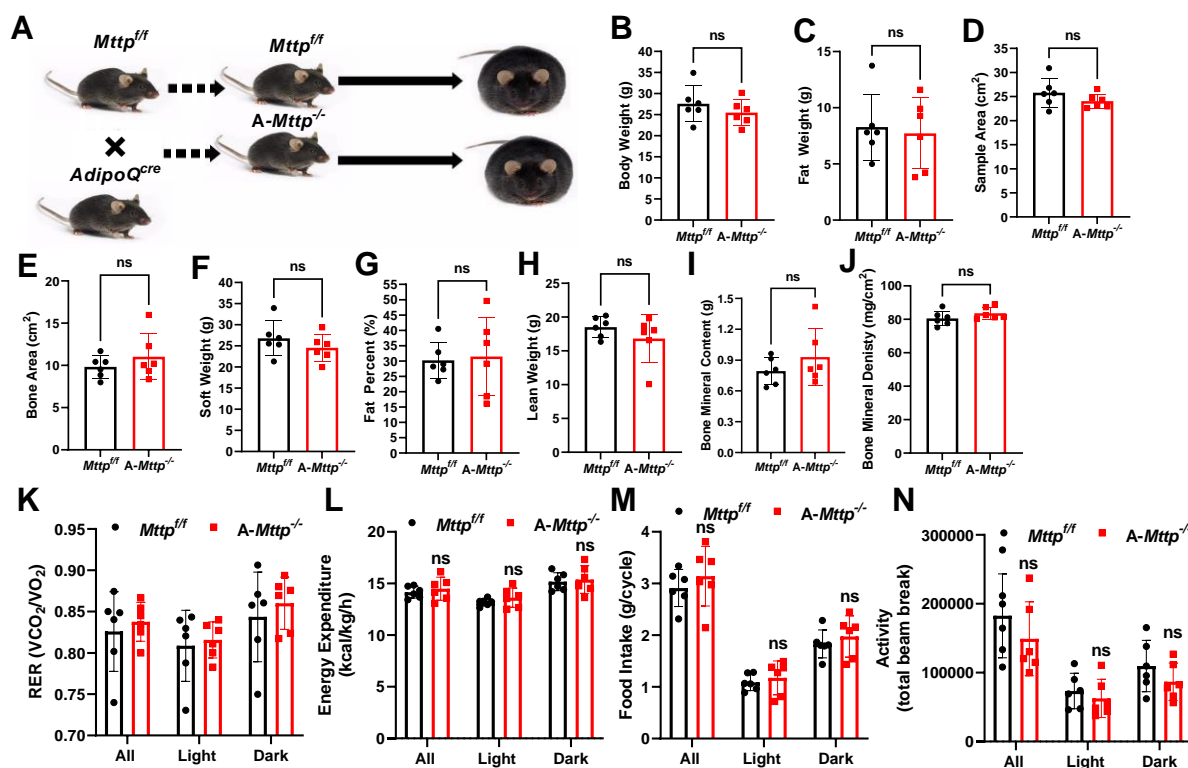


Supplementary Figure legends



Supplementary Figure 1. Comparison of MTP and apoB expression in human adipocytes and hepatoma cells.

(A-B) SVF from human omental fat was differentiated into adipocytes. Human hepatoma Huh-7 cells were cultured as described in the Methods. RNA samples were isolated and used to quantify the mRNA levels of apoB, MTP and 18S. (A) ApoB and (B) MTP mRNA levels measured by qRT-PCR in human adipocytes and Huh-7 cells. Ct values of ApoB in human adipocytes exceeded 31. Error bars represent mean \pm SD. ** $P < 0.01$, and *** $P < 0.001$ with unpaired Student's *t*-test; ns, not significant.

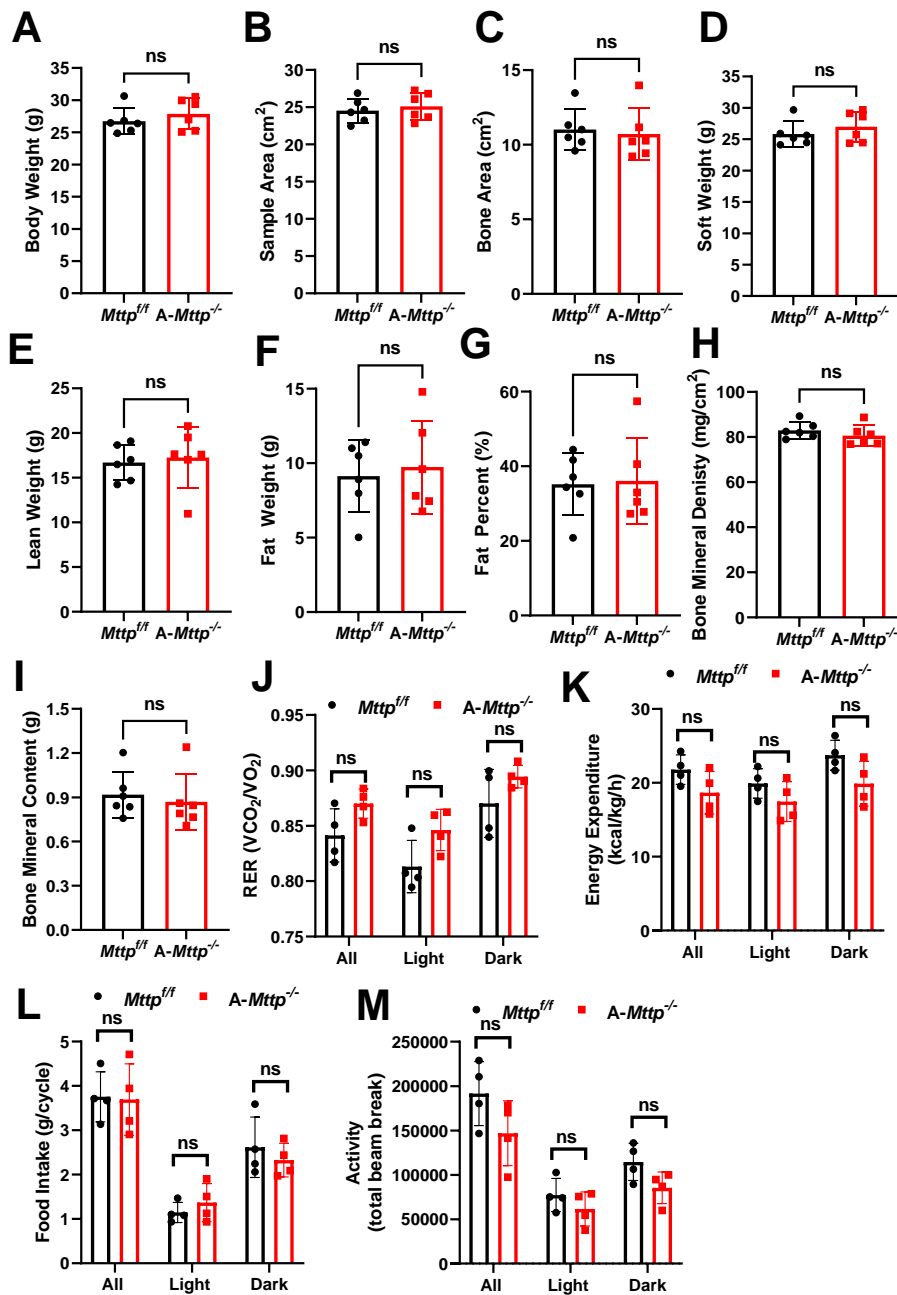


Supplementary Figure 2. Body composition and metabolic analysis of male *A-Mttp^{-/-}* mice fed a chow diet.

(A) Schematic diagram of the breeding protocol used to obtain *A-Mttp^{-/-}* and *Mttp^{f/f}* mice. *Mttp^{f/f}* mice were bred to obtain *Mttp^{f/f}* mice. In addition, they were bred with *AdipoQ^{Cre}* mice to obtain *A-Mttp^{-/-}* mice, which were then bred to obtain sufficient mice for experiments.

(B-J) Male mice (8 weeks old) were fed a chow diet for 6 months, and their body composition was analyzed with DEXA.

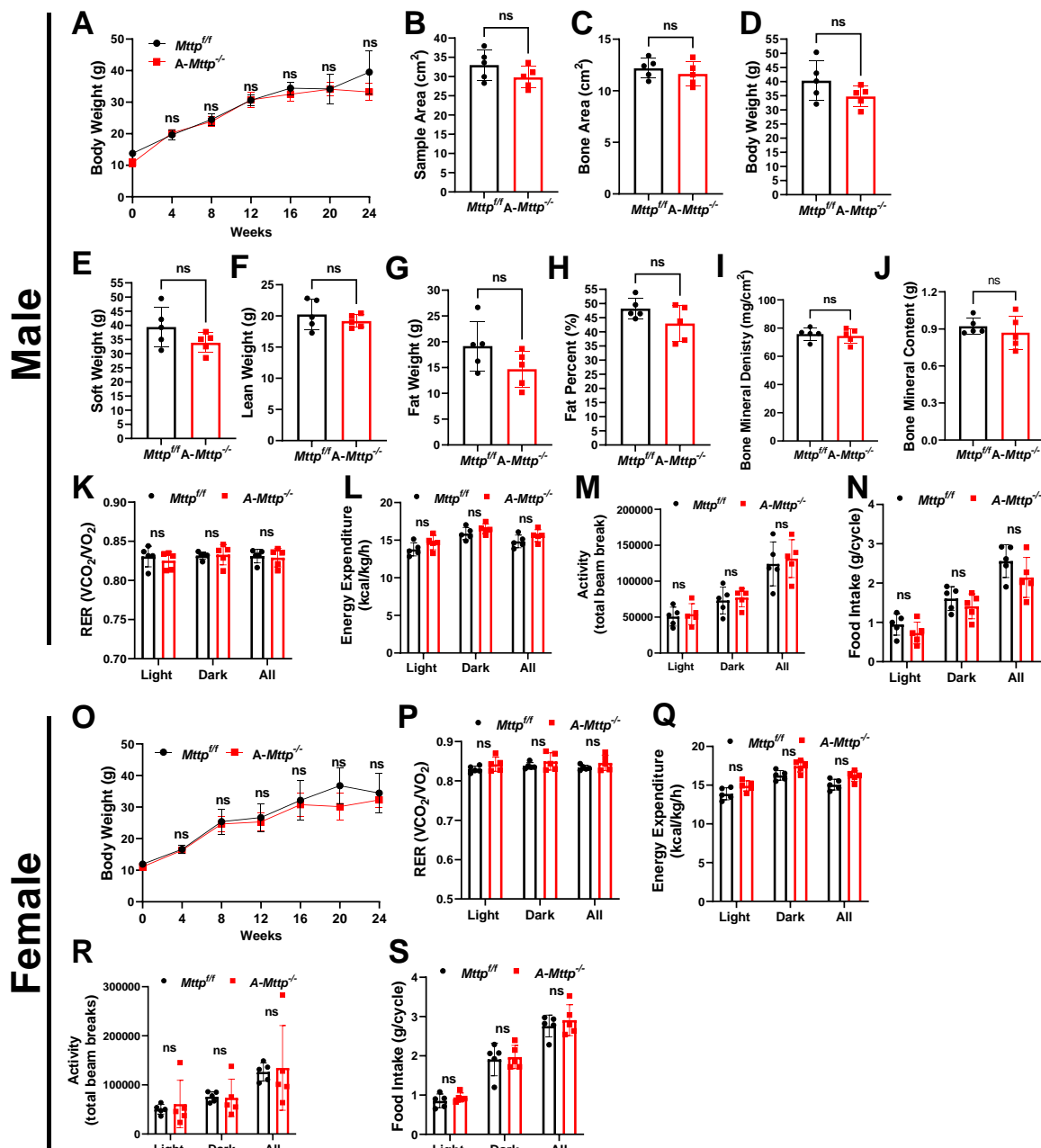
(K-N) Metabolic analysis was performed in CLAMS to measure (K) RER, (L) energy expenditure, (M) food intake and (N) Activity. Error bars represent mean \pm SD, ns $P > 0.05$. Significance calculated using unpaired Student's t test.



Supplementary Figure 3. Body composition and metabolic analysis of female *A-Mtpp*^{-/-} mice fed a chow diet.

(A-I) Female mice (8 weeks old) were fed a chow diet for 6 months, and their body composition was analyzed with DEXA.

(J-M) Metabolic analysis was performed in CLAMS to measure (J) RER, (K) energy expenditure, (L) food weight and (M) Activity. Error bars represent mean ± SD, ns P > 0.05. Significance calculated using unpaired Student's t test.

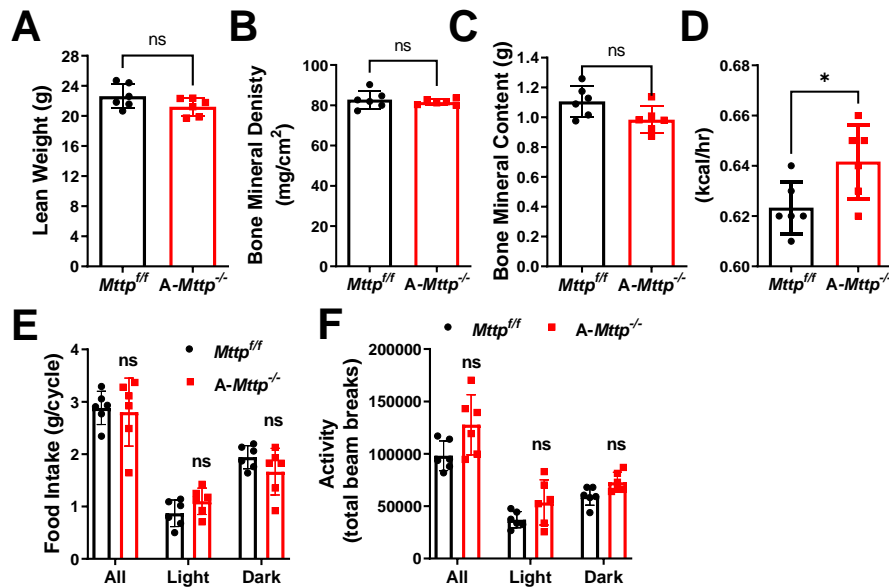


Supplementary Figure 4. Metabolic and body composition analyses of male and female *A-Mtpp^{-/-}* mice fed a 45% kcal fat diet.

(A) Male (8-week-old) mice were fed a 45% kcal fat diet, and weight gain was measured at monthly intervals. (B-J) Body composition analysis of *Mtpp^{fl/fl}* and *A-Mtpp^{-/-}* mice (n=5) after 4 months on a 45% kcal fat diet.

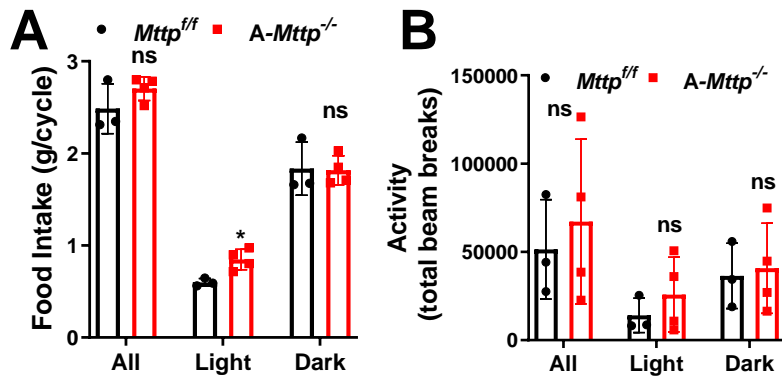
(K-N) Metabolic analysis was performed in CLAMS to measure (K) RER, (L) energy expenditure, (M) activity and (N) food intake after 5 months on diet.

(**O-S**) Female *Mttp^{ff}* and *A-Mttp^{-/-}* mice (8 weeks old) were fed a 45% kcal fat diet, and (**O**) weight gain was measured at monthly intervals. (**P**) RER, (**Q**) energy expenditure, (**R**) activity and (**S**) food intake were measured in female *Mttp^{ff}* and *A-Mttp^{-/-}* mice after 6 months on a 45% kcal fat diet. Error bars represent mean \pm SD, ns $P > 0.05$. Significance calculated using unpaired Student's t test except for graph A and O two way ANOVA followed by multiple comparison was used.



Supplementary Figure 5. *A-Mttp^{-/-}* mice show no difference in lean weight, food intake and activity.

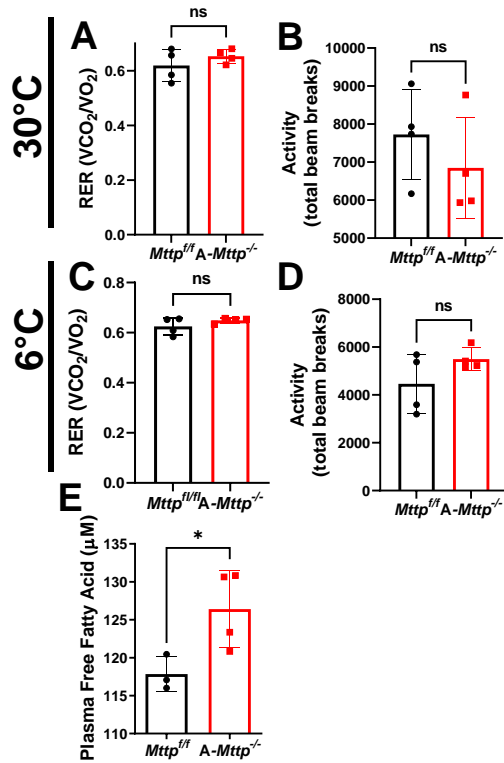
(A-D) Body composition of male *Mttp^{f/f}* and *A-Mttp^{-/-}* mice (n=6) fed an obesogenic diet for 6 months. (A) Lean weight, (B) bone mineral density (BMD) and (C) bone mineral content (BMC). Metabolic analyses of *Mttp^{f/f}* and *A-Mttp^{-/-}* mice were performed using CLAMS to measure (D) energy expenditure without normalizing with body weight, (E) food intake and (F) total activity. Error bars represent mean \pm SD, Significance was calculated with Student's t test in B-G. ns, not significant.



Supplementary Figure 6. Food intake and activity in female *A-Mttp^{-/-}* mice fed an obesogenic diet at room temperature (23°C).

Female *Mttp^{f/f}* and *A-Mttp^{-/-}* mice (12-weeks-old) were fed an obesogenic diet (60% kcal fat) for 6 months. **(A)** food intake and **(B)** activity was measured using CLAMS.

Error bars represent SD. Significance was calculated with two way ANOVA followed by multiple comparison, ns, not significant.

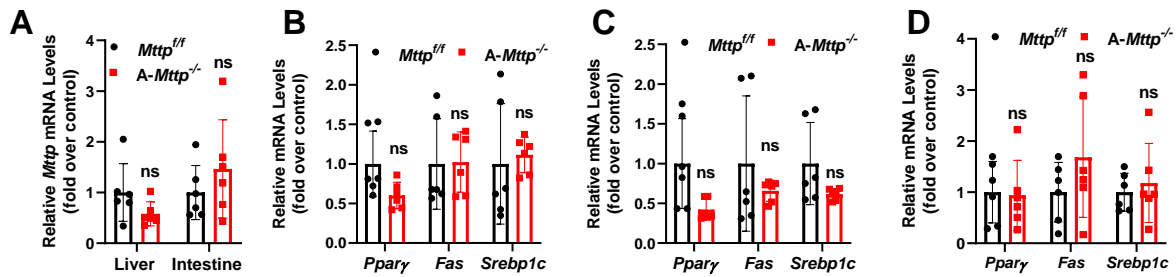


Supplementary Figure 7. Metabolic phenotypes of *Mttp^{f/f}* and *A-Mttp^{-/-}* mice at thermoneutral and cold temperatures.

(A-B) Male *Mttp^{f/f}* and *A-Mttp^{-/-}* mice (n=4) were fed an obesogenic diet for 4 months and maintained at thermo-neutral temperature (30°C) on an HFD diet for 6 weeks. Metabolic phenotyping was performed in CLAMS to measure (A) RER and (B) activity.

(C-D) Mice were kept at 6°C for 2 h, and their (C) RER and (D) activity were measured. Error bars represent SD.

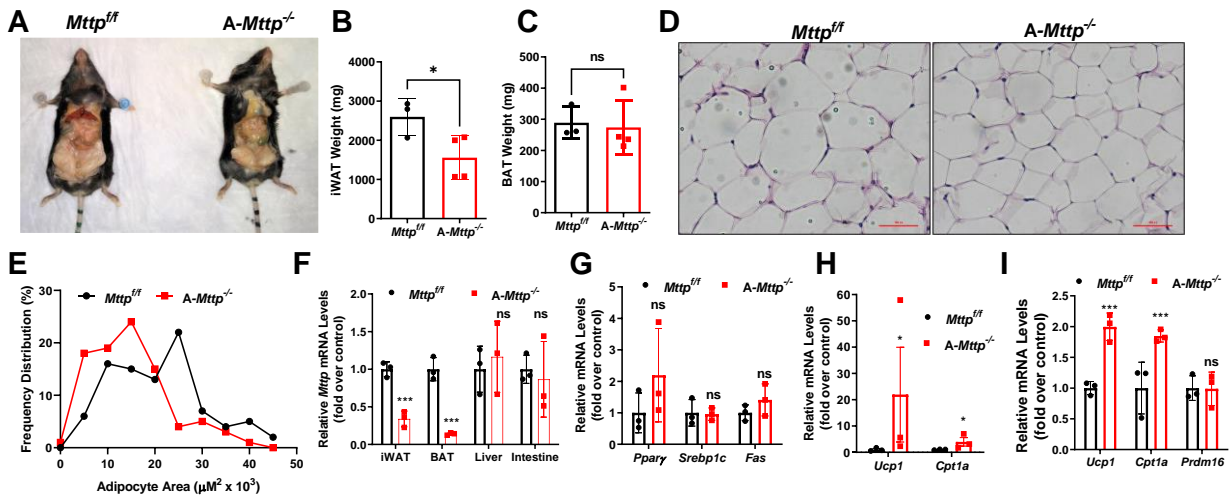
(E) Fasting plasma FFA levels in female *Mttp^{f/f}* and *A-Mttp^{-/-}* mice fed obesogenic diet for 6 months. Error bars represent SD, Significance was calculated with Student's *t*-test; *P<0.05 ns, not significant.



Supplementary Figure 8. Male *A-Mttp*^{-/-} mice show no significant differences in the expression of lipogenesis genes in iWAT, eWAT and iBAT than do *Mttp*^{ff} mice.

Mttp^{ff} and *A-Mttp*^{-/-} male mice were fed an obesogenic diet for 6 months. **(A)** Gene expression analysis of *Mttp* in the intestines and liver in *Mttp*^{ff} and *A-Mttp*^{-/-} mice.

(B-D) Expression of genes involved in adipogenesis and lipogenesis in **(B)** eWAT, **(C)** iWAT and **(D)** iBAT in *Mttp*^{ff} and *A-Mttp*^{-/-} mice (n=6). Error bars represent SD. Significance was calculated with Student's *t*-test; ns, not significant.



Supplementary Figure 9. Female *A-Mttp^{-/-}* mice have smaller adipocyte sizes and show greater expression of thermogenic genes in iWAT and iBAT than do *Mttp^{ff}* mice.

Female *Mttp^{ff}* and *A-Mttp^{-/-}* mice (12-weeks-old) were fed an obesogenic diet (60% kcal fat) for 6 months. **(A)** Representative images of *Mttp^{ff}* and *A-Mttp^{-/-}* mice (n=3–4).

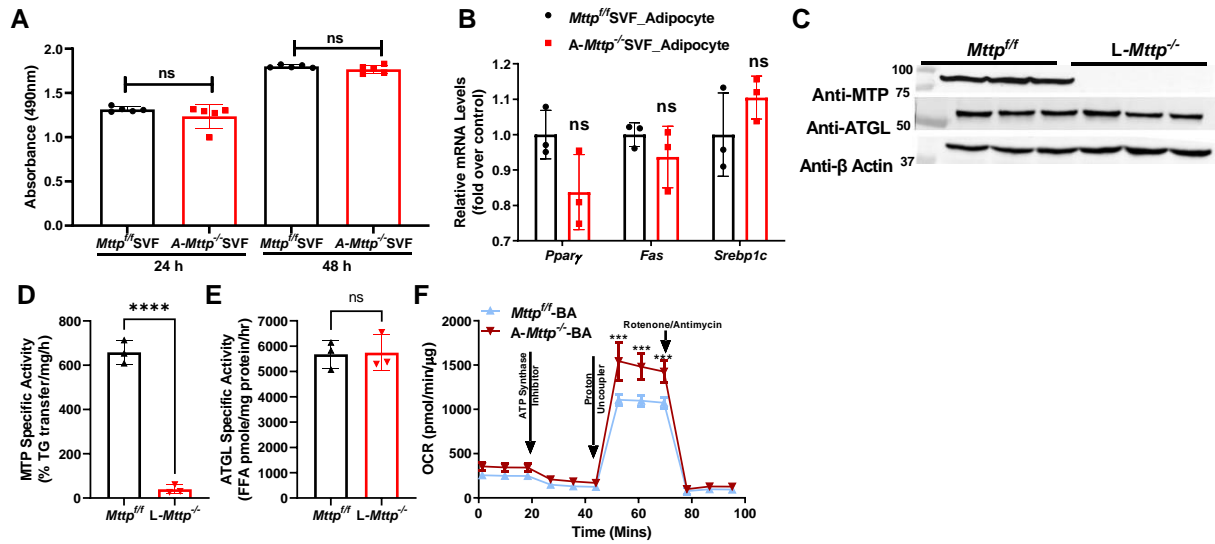
(B-C) Weights of **(B)** iWAT and **(C)** BAT of *Mttp^{ff}* and *A-Mttp^{-/-}* mice after 6 months of obesogenic diet feeding at room temperature.

(D-E) **(D)** H&E staining of iWAT. Images were taken at 20 \times magnification. Adipocyte size distribution of **(E)** iWAT in *Mttp^{ff}* and *A-Mttp^{-/-}* mice.

(F) Gene expression analysis with qRT-PCR for *Mttp* in iWAT, iBAT, liver and intestines.

(G) Expression of genes involved in adipogenesis and fatty acid synthesis in iWAT in *Mttp^{ff}* and *A-Mttp^{-/-}* mice.

(H-I) Expression of thermogenic genes in **(H)** iWAT and **(I)** iBAT of *Mttp^{ff}* and *A-Mttp^{-/-}* mice. Error bars represent SD. *P<0.05, and ***P<0.001. Significance was calculated with Student's *t*-test.



Supplementary Figure 10. MTP deficient adipocytes grow similar to WT adipocytes and show no difference in the expression of lipogenic genes.

SVF isolated from *Mttp*^{f/f} and A-*Mttp*^{-/-} mice was seeded at a density of 10,000 cells per well in 96-well cell culture plates. (A) Cell proliferation was assessed after 24 and 48 h.

(B) Gene expression analysis of *Pparγ*, *Fas* and *Srebp1c* in differentiated adipocytes.

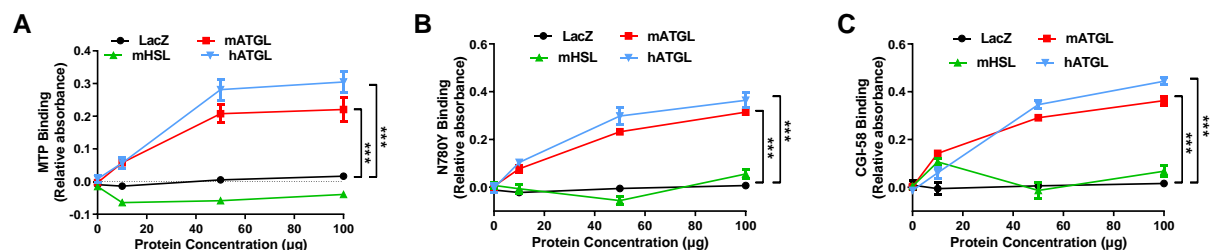
(C) Western blot analysis of MTP and ATGL in the livers of *Mttp*^{f/f} and L-*Mttp*^{-/-} mice. Actin was used as loading control.

(D) MTP activity in liver homogenates (15 μg) of *Mttp*^{f/f} and L-*Mttp*^{-/-} mice.

(E) ATGL activity in liver homogenates (50 μg) of *Mttp*^{f/f} and L-*Mttp*^{-/-} mice.

The error bars represent SD, (n= 4). Significance was calculated with Student's *t*-test. *P>0.05; ns, not significant.

(F) SVF isolated from *Mttp*^{f/f} and A-*Mttp*^{-/-} male mice were differentiated into brown adipocytes and OCR was measured in the presence of ATP synthase inhibitor, proton uncoupler and rotenone/antimycin. The error bars represent SD, (n= 3–5). Two-way ANOVA followed by multiple comparisons, ***P>0.001.



Supplementary Figure 11: MTP interacts with ATGL.

Cos-7 cells were transfected, and Flag-tagged MTP, N780Y and CGI proteins were purified. High binding plates were coated with purified (A) MTP, (B) N780Y or (C) CG-I58. These plates were incubated with different concentrations of lysates of Cos-7 cells expressing His-tagged LacZ (control), hATGL, mATGL and HSL. Binding of proteins was detected with anti-His primary antibody and secondary antibodies conjugated with horseradish peroxidase. The absorbance of the peroxidase reaction was determined at 450 nm. The data are representative of three to five independent experiments, each containing three biological replicates. Significance was calculated with two-way ANOVA, ***P<0.001.